Asian Journal of Chemistry; Vol. 33, No. 10 (2021), 2321-2326

ASIAN JOURNAL OF CHEMISTRY

https://doi.org/10.14233/ajchem.2021.23321

Reduced Graphene Oxide-Resorcinol Nanocomposite: A Chemosensor for the Detection of Cerium Ions

DAVID JOHN DMONTE[1,2], A. PANDIYARAJAN[2,3], RAJESH SWAMINATHAN[4], SAKUNTHALA AYYASAMY[4], VIDHYA BHOJAN[2,*] and RAJU NANDHAKUMAR[5,*]

[1]Centre of Polymer Systems, University Institute, Tomas Bata University in Zlin, Trida Tomase Bati 5678, 760 01 Zlin, Czech Republic
[2]Centre for Nanoscience and Genomics, Karunya Institute of Technology and Sciences (Deemed to be University), Coimbatore-641114, India
[3]Department of Materials Science and Engineering, National Dong Hwa University, Shoufeng, 974 01 Hualien, Taiwan
[4]Department of Applied Physics, Karunya Institute of Technology and Sciences (Deemed to be University), Coimbatore-641114, India
[5]Department of Applied Chemistry, Karunya Institute of Technology and Sciences (Deemed to be University), Coimbatore-641114, India

*Corresponding authors: E-mail: vidhya@karunya.edu; nandhakumar@karunya.edu

Received: 19 May 2021; *Accepted*: 9 July 2021; *Published online*: 20 September 2021; AJC-20501

A hybrid material reduced graphene oxide based organic nanocomposite was synthesized from graphite by modified Hummers method, which is further chemically reduced to form reduced graphene oxide (rGO) and with resorcinol through a solvothermal process a reduced graphene oxide-resorcinol (rGO-R) nanocomposite was obtained. The synthesized materials surface morphology and structural compositions were studied through X-ray diffraction (XRD) and scanning electron microscope (SEM) and their optical properties were studied through UV-visible spectroscopy and photoluminescence. The material was further used as a fluorescent chemosensor to detect cerium ion under aqueous conditions. The rGO-R composite's sensing abilities were studied by following parameters *viz.* pH, reversibility, time and the interference of other probable competing ions. The sensing follows both the photo-induced electron transfer and intramolecular charge transfer processes.

Keywords: Reduced graphene oxide, Resorcinol, Nanocomposite, Chemosensor, Cerium.

INTRODUCTION

Cerium, a most abundant rare earth element, needs to be studied more to better understand the properties of lanthanides [1-4]. It has been extensively used in industry and science because of its availability [5,6] and recently the potential in many various applications such as chlorophyll formation, antibacterial activity and osteoclast genesis was discovered [7-9]. Cerium ion has improved adhesion, luminescence properties and decay kinetics, which increases its attraction towards various fields of research to explore its potential applications [10,11]. Various compounds of cerium play a vital part in human physiology [12]. Its usage as micro fertilizer in the agricultural industry has spiked a lot of interest [13,14]. On the other hand, cerium is documented to have several harmful effects on human skin depending on its contact and frequency [15]. It is known to have negative effects on an aquatic ecosystem on account of being detrimental to cells [16]. Hence, detection and quantification of cerium ion in aqueous media is a important factor. Even though an effective methodology to sense reactive lanthanide and rare earth metal such as cerium is already present, it still lacks ease and efficiency.

Among the chemical sensors, metal oxide nanomaterials have recently been in high demand because of their desirable properties such as high sensitivity, small size, cost and power efficient [17,18]. Recently, in this field graphene quantum dots (GQDs) have been synthesized and utilized by Salehnia *et al.* [19] to detect cerium ions in aqueous solution. This synthetization process was used to obtain a hybrid graphene oxide resorcinol composite to detect Ce^{3+} ion in aqueous solution [20]. Recently, few reports on the sensing of cerium ion has been reported through various mechanisms such as fluorescence "on-off" change, aggregation-induced emission (AIE), ratiometric sensing, *etc.* [21-25]. Graphene has been exploited in many fields of research due to its excellent properties such as electrical conductivity [26-29], optical activity [30,31] and

mechanical strength [32,33]. The photo luminescent property possesses is a novel area of study for future applications. Reduced graphene oxide (rGO) is known to be water dispersible and still having possible realistic properties to ideal graphene when compared to the other materials in the graphene family [34]. The oxygen-comprised functional groups and the few oxidized sp^3 sites contribute to fluorescence, allowing for tunable emission wavelength based on the sp^2 plane [35]. Over time, various types of sensors have been fabricated using graphene for monitoring the environment and health. In this work, we intend to prepare an advanced fluorescent chemosensor based on a reduced graphene oxide resorcinol (rGO-R) nanocomposite with a high performance in sensing cerium ions in aqueous solution. The sensing behaviour of the material shows that it may be used to fabricate sensing devices to be better than current colorimetric sensors while being cost effective, fast and reversible.

EXPERIMENTAL

The precursors, graphite and resorcinol were procured from Aldrich and all other chemicals and commonly available solvents were purchased from Merck. To detect absorption spectra, a Shimadzu UV-240 spectrophotometer was used. FT-IR studies were recorded on Shimadzu Prestige-20 IR Spectrometer. Scanning electron microscope (SEM) studies were carried out on JEOL model JSM-6390 and SHIMADZU model XRD-6000 was used to perform X-ray diffraction (XRD). Fluorescence measurements were taken on a Jasco FP-8200 spectrofluorometer equipped with quartz cuvettes of 1 cm path length. All absorption and emission spectra were recorded at 25 ± 1 ºC. Stock solutions for analysis were prepared at the concentration of 2×10^{-3} M for all the metal ions immediately before the experiments. The solutions of metal ions were prepared from nitrate salts of Na^+, K^+, Al^{3+}, Cu^{2+}, Cd^{2+}, La^{3+}, Pb^{2+}, Zn^{2+}, Co^{2+}, Ni^{2+}, Ca^{2+}, Mn^{2+}, Cr^{3+}, Ba^{2+}, Ce^{3+}, Mg^{2+}, Fe^{2+}, Fe^{3+}, Hg^{2+} and Ag^+.

Synthesis of reduced graphene oxide resorcinol nanocomposite (rGO-R): The graphene oxide (GO) was prepared by a modified Hummers method [36]. It was converted to reduced graphene oxide (rGO) by using the sodium borohydride as a reducing agent [37]. Graphene oxide (GO, 0.3 g) was dispersed in 100 mL of deionized water and sonicated until particulate matter could not be observed. Then, sodium borohydride (0.4 g) was added and the mixture was heated in an oil bath at 100 ºC for 24 h. The rGO sample was obtained by repeated centrifugation with deionized water. Further, resorcinol doped was done in 1:1 ratio [38]. First 500 mg of rGO was dissolved in 100 mL distilled water and sonicated for 0.5 h to make a clear solution. Resorcinol (500 mg) was dissolved in distilled water and sonicated for 0.5 h separately to make a clear solution. After that these two solutions were mixed, transferred to 250 mL round-bottomed flask and kept under reflux (80 ºC) for 24 h as a hydrothermal process. The resultant solution was filtered and kept in hot air oven at 60 ºC for an additional 24 h. Then, the water was fully evaporated and dried to obtain the desired reduced graphene oxide resorcinol nanocomposite (rGO-R).

RESULTS AND DISCUSSION

Reduced graphene oxide resorcinol nanocomposite (rGO-R) was prepared by a two step protocol as shown in **Scheme-I**. Firstly, the graphene oxide was converted to reduced graphene oxide (rGO). Secondly, the rGO and resorcinol were mixed

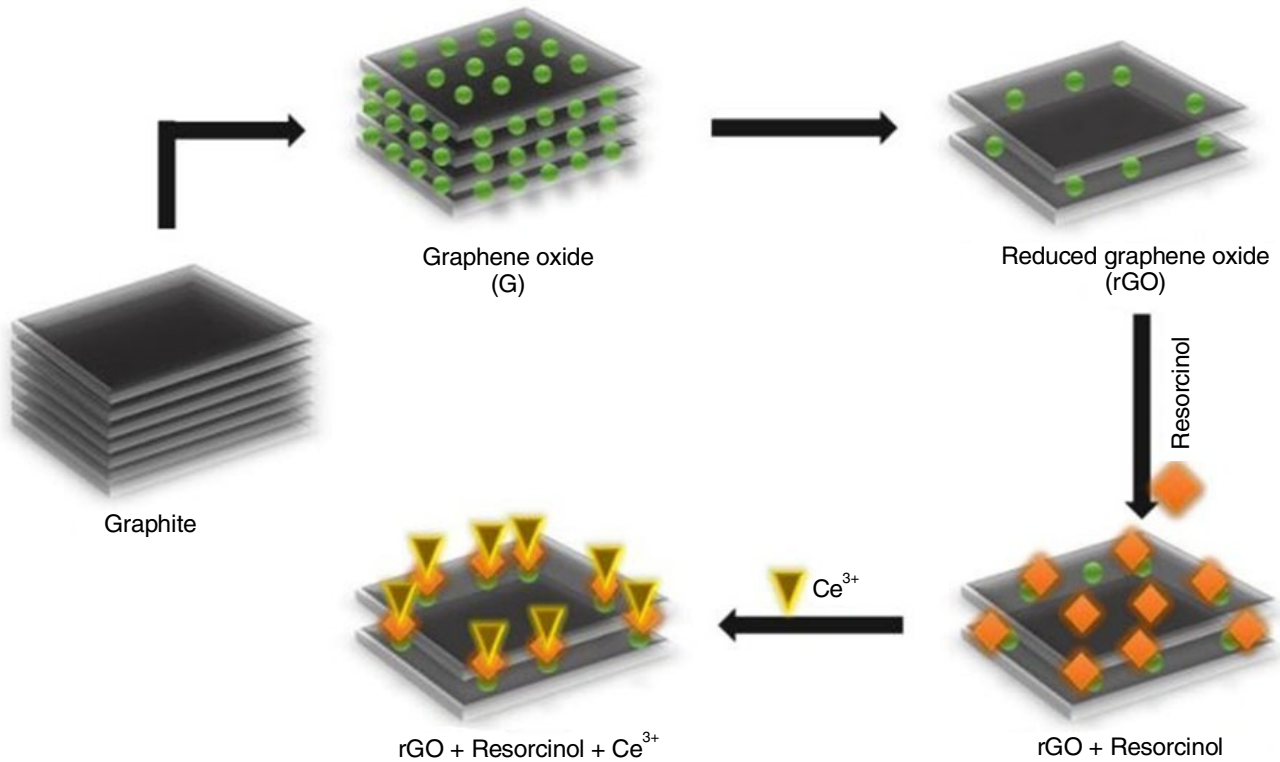

Scheme-I: Synthesis of rGO-R nanocomposite and sensing of cerium ions

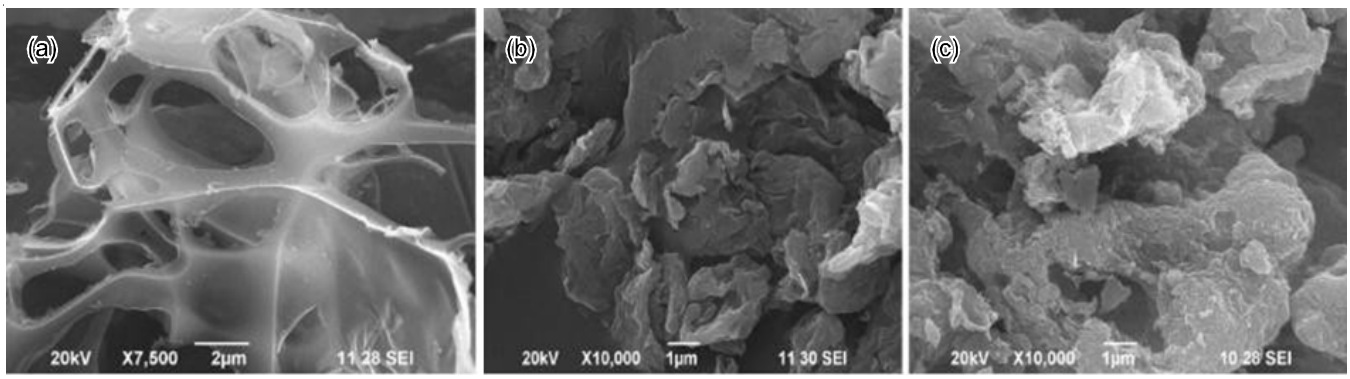

Fig. 1. SEM images: (a) resorcinol (b) reduced graphene oxide (c) reduced graphene oxide-resorcinol (rGO-R) nanocomposite

under hydrothermal conditions to obtain the desired reduced graphene oxide resorcinol nanocomposite (rGO-R).

SEM studies: Fig. 1 explains the various observed morphological features in the images. The SEM images show the surface morphology of resorcinol as flakes and reduced graphene oxide (rGO) as sheets. However, in the case of rGO-R, it is clearly observed that the resorcinol flakes are densely adsorbed on the surface of the reduced graphene oxide sheets, which proves that the resorcinol flakes are adsorbed without causing any topological changes with the graphene sheets.

FTIR studies: The FTIR spectra show peaks at 1810 cm^{-1} as stretching vibrations for C=O (Fig. 2) in the case of rGO. The peaks for C-OH and C-O stretching vibrations exhibit at 1560 and 1126 cm^{-1}, respectively and seem to remain intact, which is caused by remaining carboxyl groups even after chemical reduction [39]. A very broad peak at 3215 cm^{-1} is attributed to the O-H moiety and sharp peaks at 1617 cm^{-1} signifies the C=C bonding in resorcinol. Nevertheless, for rGO-R nanocomposite the peak is observed at 1607 cm^{-1}, a shift from 1617 cm^{-1} may be due to the hydrogen bonding between the –OH of resorcinol and remaining –C=O of the rGO. Therefore, the FT-IR spectra revealed that the resorcinol molecules were substantially adsorbed on the surface of the rGO sheets forming the rGO-R nanocomposite.

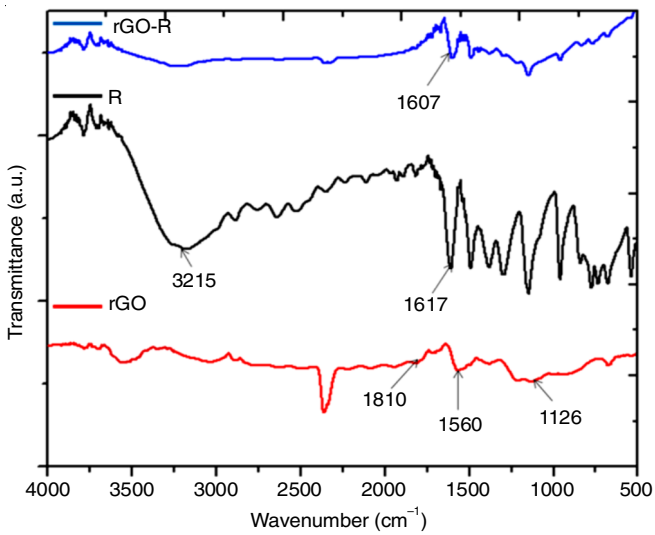

Fig. 2. FTIR spectra of resorcinol, reduced graphene oxide and reduced graphene oxide-resorcinol (rGO-R) nanocomposite

UV-visible studies: The interaction between resorcinol and rGO was examined by absorbance spectra as shown in Fig. 3. The absorption peak of free resorcinol has high intensity and broad in nature. However, the rGO-R UV spectra shows slightly broadened peak with low intensity on comparison with resorcinol and no notable shift in the peaks were also observed. This is suggestive of the π-π interactions between the rGO and resorcinol.

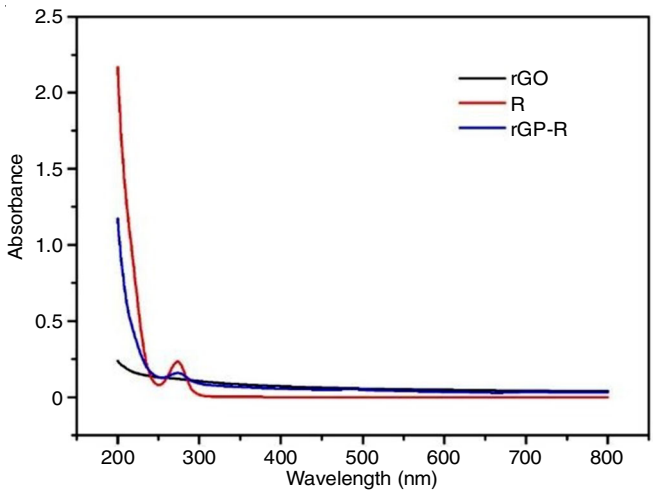

Fig. 3. UV spectra of resorcinol, reduced graphene oxide and reduced graphene oxide-resorcinol (rGO-R) nanocomposite

XRD studies: In Fig. 4, the XRD pattern of rGO exhibits a strong peak at 2θ = 25º, which correlates to the reduction of oxygen functionalities and the distance between the graphene layers. As can be seen, the diffraction peak at 2θ = 43º indicates the short-range order of stacked graphene layers. The same diffraction peaks can be observed in the case of the rGO-R nano composites along with additional broad peaks of resorcinol around 2θ = 18º. This shows that the resorcinol scaffold is non-covalently adsorbed on the surface of rGO to form the rGO-R nanocomposites.

Fluorescence studies

Metal selectivity spectrum of rGO-R nanocomposite: The synthesized chemosensor, rGO-R was utilized for the detection of biologically and environmentally important metal ions. Accordingly, rGO-R nanocomposite stock solution (2×10^{-3} M) was prepared in partial aqueous media under the physio-

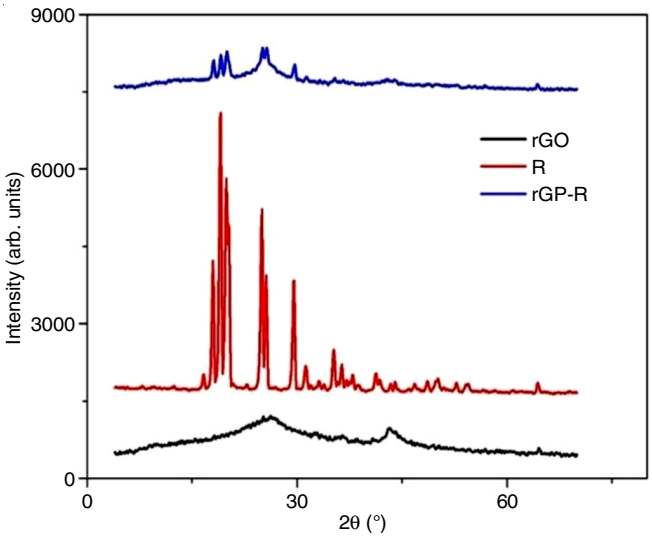

Fig. 4. XRD spectra of resorcinol, reduced graphene oxide and reduced graphene oxide-resorcinol (rGO-R) nanocomposite

logical pH and it was diluted to the required concentration. All the metals ions were prepared in 2×10^{-3} M in aqueous medium. The final solution of the rGO-R nanocomposite and metal ions was excited at 273 nm and the spectra were recorded. The interaction of synthesized rGO-R with metal cations was studied by fluorescent spectroscopy. The rGO-R receptor solution (THF-H_2O, 1:1 v/v, HEPES 50 mM, pH = 7.4) in the presence of various metal ions (100 equiv. of each, excited at 273 nm) gave a significant fluorescence enhancement with an emission maximum at 306 nm during the addition of Ce^{3+} to the solution. Interestingly, this also led to a noteworthy red shift of the fluorescence intensity to 351 nm from 306 nm, while it only produced indistinctive changes for other potentially competing metal ions in the metal selectivity fluorescence spectra (Fig. 5) [40].

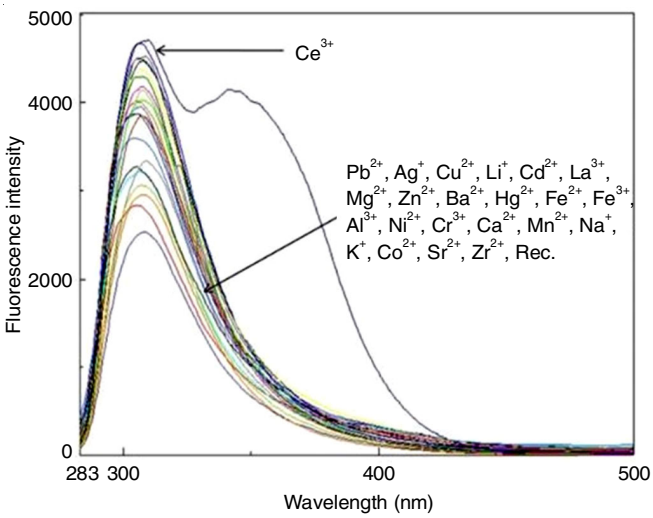

Fig. 5. Fluorescence changes of rGO-R nanocomposite (THF-H_2O, 1:1 v/v, HEPES 50 mM, pH = 7.4) in the presence of various metal ions (100 equiv. of each, excited at 273 nm)

Interference of Ce^{3+} with other metal ions: The interferences by various other metal ions during the detection of cerium ions were examined through competitive complexation experiments [41]. The fluorescence change was recorded by the treatment of 100 equiv. of Ce^{3+} ions in the presence of equiv. of other interfering metal ions. From Fig. 6, it is clear that there are no prominent fluorescence changes in the receptor rGO-R nanocomposite solution (THF-H_2O, 1;1 v/v, HEPES = 50 mM, pH = 7.4) in the presence of various metal ions (100 equal of each, excited at 273 nm, emission at 283 nm) during the detection of cerium ions. These results suggest that receptor rGO-R can be used for the selective detection of Ce^{3+} ion in real sample analysis.

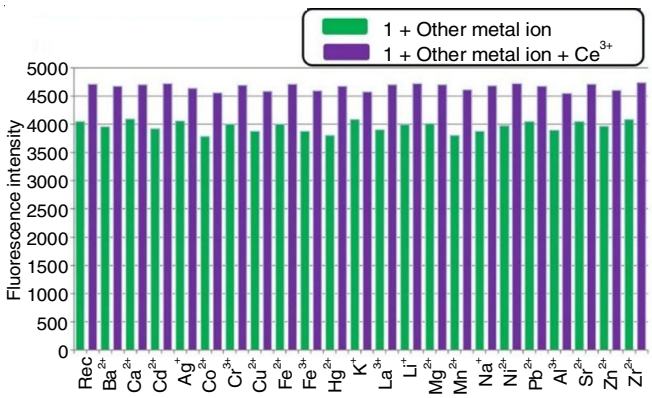

Fig. 6. Fluorescence changes of receptor rGO-R (THF-H_2O, 1:1 v/v, HEPES 50 mM, pH = 7.4) in the presence of various metal ions (100 equiv. of each, excited at 273 nm)

Fluorescence changes with various equivalent Ce^{3+}: In Fig. 7, the fluorescence intensity of receptor rGO-R (THF-H_2O, 1:1 v/v, HEPES 50 mM, pH=7.4) along with the addition of different amounts of Ce^{3+} (0-100 equivalent excited at 273 nm) was recorded. It is clearly seen that during the addition of Ce^{3+} (0-100 equivalent), the fluorescent intensity gradually increases and gets saturated during the addition of 100 equivalents along with a remarkable bathochromic peak shift. The results suggested that the fluorescence changes being observed are directly proportional. This notable red shift may

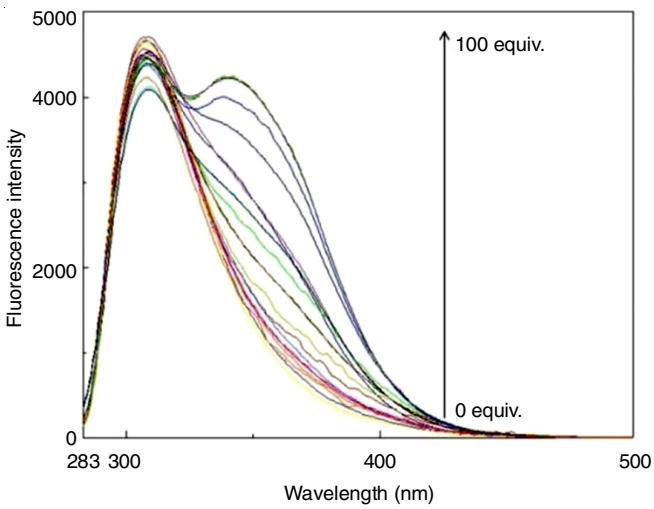

Fig. 7. Fluorescence titration of rGO-R (THF-H_2O, 1;1 v/v, HEPES = 50 mM, pH = 7.4) solution upon the addition of various equivalent of Ce^{3+} (0-100 equiv.) (λ_{ex} = 273 nm, λ_{em} = 283 nm)

possibly be due to the blocking of the lone pair of electrons from the oxygen atoms which are responsible for the photo-induced electron transfer (PET) quenching. Hence, there takes place the intramolecular charge transfer (ICT) between the reduced graphene oxide and resorcinol scaffolds [42].

Time and pH effect: The fluorescence intensity changes for rGO-R and rGO-R+Ce^{3+} in THF-H_2O solution (1:1 v/v) at different pH values (λ_{ex} = 273 nm) are shown in Fig. 8. The fluorescence intensity is not quite stable for the receptor between the pH range of 3 to 11, constant quenching and enhancements are noted. This may be probably due to the protonation and deprotanation of the free rGO-R receptor [43]. However, the fluorescence intensity of rGO-R+Ce^{3+} complex is relatively stable at a pH range 7 to 9 with enhanced fluorescence intensity. Hence, the physiological pH of 7.4 was chosen for all the experiments.

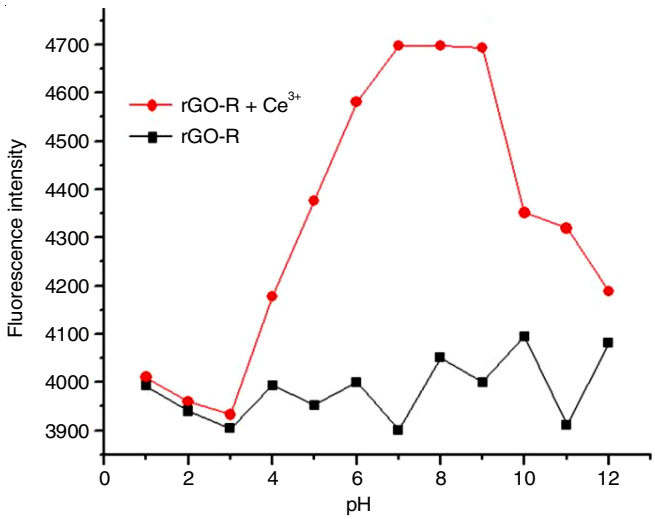

Fig. 8. pH effect of rGO-R and rGO-R + Ce^{3+} in THF-H_2O solution (1:1 v/v, HEPES 50 mM, pH = 7.4) (excited at 273 nm)

Furthermore, for any chemosensor the effective time is more important for practical applications. Therefore, changes in fluorescence intensities of rGO-R to Ce^{3+} (THF-H_2O, 1;1 v/v, HEPES 50 mM, pH = 7.4) against time was examined. As shown in Fig. 9 the fluorescence intensity of the receptor increases with a red shift and reaches the maximum level of saturation within 2 min. It remains steady for further 10 min upon the addition of Ce^{3+} ions to chemosensor rGO-R. This indicates that the chemosensor rGO-R selectively detects Ce^{3+} ion in a short span of time [44].

Reversibility of receptor + Ce^{3+}: The analysis for the reversibility of the binding between the chemosensor rGO-R and Ce^{3+} in the presence of EDTA in THF-H_2O solution (1:1 v/v, HEPES 50 mM, pH = 7.4, excited at 273 nm) was conducted with utmost precision. From Fig. 10, the disappearance of the fluorescence signals of rGO-R and Ce^{3+} can be seen on addition of EDTA. This highlights the chelation process between Ce^{3+} with EDTA, which on successful repetition proves to be reversible and completes within 2 min. The reciprocation showed that it can utilize present probe more than 8 cycles for the sensing of Ce^{3+} ion [45].

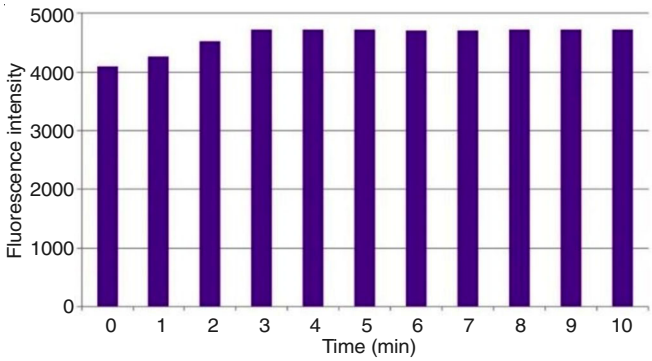

Fig. 9. Effective time response of receptor rGO-R + Ce^{3+} in THF-H_2O solution (1:1 v/v, HEPES 50 mM, pH = 7.4) (excited at 273 nm)

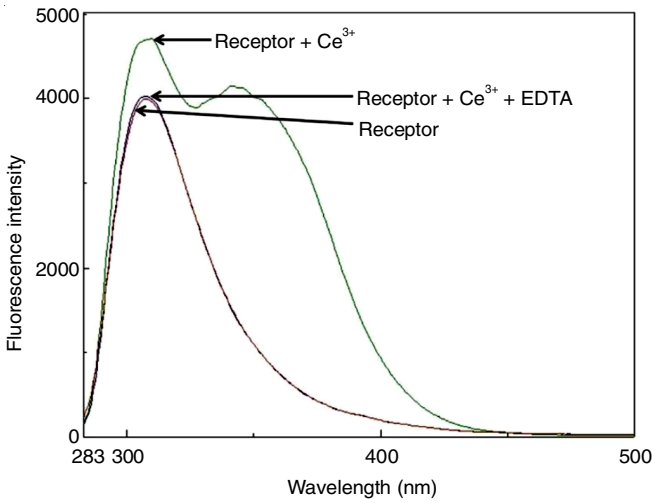

Fig. 10. Reversibility of receptor rGO-R + Ce^{3+} in the presence of EDTA in THF-H_2O solution (1:1 v/v, HEPES 50 mM, pH = 7.4, excited at 273 nm)

Conclusion

In this work, synthesized reduced graphene oxide was incorporated with organic scaffold, resorcinol (rGO-R). The novel chemosensor rGO-R was characterized by analytical, spectroscopic and microscopic techniques which included IR, SEM, UV-vis, fluorescence and XRD. The interactions between the chemosensor rGO-R and the metal ions were studied in detail. The newly prepared chemosensor rGO-R had very good selectivity for cerium ions, even among interference of other competing metal ions, showed promising reusable fluorescence activity over time, even in varying pH conditions. The selectivity of cerium ions by the receptor rGO-R takes place due to the arrest of photoinduced electron transfer process (PET) which facilitates the intramolecular charge transfer (ICT) process which eventually led to a bathochromic shift. Therefore, the above studies pave a path for future applications of rGO as a key player in the development of fluorescent chemosensors festooned with organic fluorophores. Further works on the construction of rGO-organic hybrids are also underway.

ACKNOWLEDGEMENTS

This work is supported by the SERB-EMR grant by the DST (Sanction No. SERB-EMR/2016/005692). Center for

Research in Nanotechnology, Karunya Institute of Technology and Sciences, Coimbatore, India supported the characterization techniques.

CONFLICT OF INTEREST

The authors declare that there is no conflict of interests regarding the publication of this article.

REFERENCES

1. M.R. Awual, M.M. Hasan, A. Shahat, M. Naushad, H. Shiwaku and T. Yaita, *Chem. Eng. J.*, **265**, 210 (2015); https://doi.org/10.1016/j.cej.2014.12.052
2. M.R. Awual, T. Kobayashi, H. Shiwaku, Y. Miyazaki, R. Motokawa, S. Suzuki, Y. Okamoto and T. Yaita, *Chem. Eng. J.*, **225**, 558 (2013); https://doi.org/10.1016/j.cej.2013.04.015
3. M.R. Awual, T. Kobayashi, Y. Miyazaki, R. Motokawa, H. Shiwaku, S. Suzuki, Y. Okamoto and T. Yaita, *J. Hazard. Mater.*, **252-253**, 313 (2013); https://doi.org/10.1016/j.jhazmat.2013.03.020
4. M.R. Awual, N.H. Alharthi, Y. Okamoto, M.R. Karim, M.E. Halim, M.M. Hasan, M.M. Rahman, M.M. Islam, M.A. Khaleque and M.C. Sheikh, *Chem. Eng. J.*, **320**, 427 (2017); https://doi.org/10.1016/j.cej.2017.03.075
5. S. Sarkar, C.M. Chatti, V.N.K.B. Adusumalli and V. Mahalingam, *ACS Appl. Mater. Interfaces*, **7**, 25072 (2015); https://doi.org/10.1021/acsami.5b06730
6. H.A. Zamani, N.R. Ganjali and M. Adib, *Sens. Actuators B Chem.*, **120**, 545 (2007); https://doi.org/10.1016/j.snb.2006.03.013
7. H. Fashui, W. Ling, M. Xiangxuan, W. Zheng and Z. Guiwen, *Biol. Trace Elem. Res.*, **89**, 263 (2002); https://doi.org/10.1385/BTER:89:3:263
8. Y. Kuang, X. He, Z. Zhang, Y. Li, H. Zhang, Y. Ma, Z. Wu and Z. Chai, *J. Nanosci. Nanotechnol.*, **11**, 4103 (2011); https://doi.org/10.1166/jnn.2011.3858
9. L. Zhou, S. Tang, L. Yang, X. Huang, L. Zou, Y. Huang, S. Dong, X. Zhou and X. Yang, *J. Trace Elem. Med. Biol.*, **52**, 126 (2019); https://doi.org/10.1016/j.jtemb.2018.12.006
10. M.S. Li and P.Y. Hou, *Acta Mater.*, **55**, 443 (2007); https://doi.org/10.1016/j.actamat.2006.07.047
11. N.R. Panda, B.S. Acharya, T.B. Singh and R.K. Gartia, *J. Lumin.*, **136**, 369 (2013); https://doi.org/10.1016/j.jlumin.2012.12.002
12. V. Höllriegl, M. González-Estecha, E.M. Trasobares, A. Giussani, U. Oeh, M.A. Herraiz and B. Michalke, *J. Trace Elem. Med. Biol.*, **24**, 193 (2010); https://doi.org/10.1016/j.jtemb.2010.03.001
13. J.T. Dahle and Y. Arai, *Int. J. Environ. Res. Public Health*, **12**, 1253 (2015); https://doi.org/10.3390/ijerph120201253
14. D. Li, S. Huang, W. Wang and A. Peng, *Chemosphere*, **44**, 663 (2001); https://doi.org/10.1016/S0045-6535(00)00357-X
15. J. Emsley, Nature's Building Blocks: Everything You Need to Know about the Elements, Oxford University Press (2011).
16. B.M. Angel, P. Vallotton and S.C. Apte, *Aquat. Toxicol.*, **168**, 90 (2015); https://doi.org/10.1016/j.aquatox.2015.09.015
17. V. Galstyan, E. Comini, A. Ponzoni, V. Sberveglieri and G. Sberveglieri, *Chemosensors*, **4**, 6 (2016); https://doi.org/10.3390/chemosensors4020006
18. E. Comini, G. Faglia and G. Sberveglieri, Solid State Gas Sensing, Springer US, Boston, MA (2009).
19. F. Salehnia, F. Faridbod, A.S. Dezfuli, M.R. Ganjali and P. Norouzi, *J. Fluoresc.*, **27**, 331 (2017); https://doi.org/10.1007/s10895-016-1962-5
20. D.J. Dmonte, A. Pandiyarajan, N. Bhuvanesh, R. Nandhakumar and S. Suresh, *Mater. Lett.*, **227**, 154 (2018); https://doi.org/10.1016/j.matlet.2018.05.051
21. M. Liu, Z. Xu, Y. Song, H. Li and C. Xian, *J. Lumin.*, **198**, 337 (2018); https://doi.org/10.1016/j.jlumin.2018.02.047
22. X. Li, Y. Zheng, Y. Tang, Q. Chen, J. Gao, Q. Luo and Q. Wang, *Spectrochim. Acta A Mol. Biomol. Spectrosc.*, **206**, 240 (2019); https://doi.org/10.1016/j.saa.2018.08.021
23. Y. Wang, X. Pan, Z. Peng, Y. Zhang, P. Liu, Z. Cai, B. Tong, J. Shi and Y. Dong, *Sens. Actuators B Chem.*, **267**, 351 (2018); https://doi.org/10.1016/j.snb.2018.04.056
24. M. Panchal, A. Kongor, M. Athar, V. Mehta, P.C. Jha and V.K. Jain, *New J. Chem.*, **42**, 311 (2018); https://doi.org/10.1039/C7NJ02828H
25. F. Nemati and R. Zare-Dorabei, *Talanta*, **200**, 249 (2019); https://doi.org/10.1016/j.talanta.2019.03.059
26. X. Li, X. Wang, L. Zhang, S. Lee and H. Dai, *Science*, **319**, 1229 (2008); https://doi.org/10.1126/science.1150878
27. C. Di, D. Wei, G. Yu, Y. Liu, Y. Guo and D. Zhu, *Adv. Mater.*, **20**, 3289 (2008); https://doi.org/10.1002/adma.200800150
28. S. Pang, H.N. Tsao, X. Feng and K. Mullen, *Adv. Mater.*, **21**, 3488 (2009); https://doi.org/10.1002/adma.200803812
29. Z.-S. Wu, S. Pei, W. Ren, D. Tang, L. Gao, B. Liu, F. Li, C. Liu and H.-M. Cheng, *Adv. Mater.*, **21**, 1756 (2009); https://doi.org/10.1002/adma.200802560
30. E.J. Yoo, T. Okata, T. Akita, M. Kohyama, J. Nakamura and I. Honma, *Nano Lett.*, **9**, 2255 (2009); https://doi.org/10.1021/nl900397t
31. Y. Xu, Z. Liu, X. Zhang, Y. Wang, J. Tian, Y. Huang, Y. Ma, X. Zhang and Y. Chen, *Adv. Mater.*, **21**, 1275 (2009); https://doi.org/10.1002/adma.200801617
32. S. Chuah, Z. Pan, J.G. Sanjayan, C.M. Wang and W.H. Duan, *Constr. Build. Mater.*, **73**, 113 (2014); https://doi.org/10.1016/j.conbuildmat.2014.09.040
33. L.C. Tang, Y.J. Wan, D. Yan, Y.B. Pei, L. Zhao, Y.B. Li, L.B. Wu, J.X. Jiang and G.Q. Lai, *Carbon*, **60**, 16 (2013); https://doi.org/10.1016/j.carbon.2013.03.050
34. Y. Chen, J. Qian, X. Liu, Q. Zhuang and Z. Han, *New J. Chem.*, **37**, 2500 (2013); https://doi.org/10.1039/c3nj00355h
35. J. Shang, L. Ma, J. Li, W. Ai, T. Yu and G.G. Gurzadyan, *Sci. Rep.*, **2**, 792 (2012); https://doi.org/10.1038/srep00792
36. L. Shahriary and A. Athawale, *Int. J. Renew. Energy Environ. Eng.*, **2**, 58 (2014).
37. L.G. Guex, B. Sacchi, K.F. Peuvot, R.L. Andersson, A.M. Pourrahimi, V. Ström, S. Farris and R.T. Olsson, *Nanoscale*, **9**, 9562 (2017); https://doi.org/10.1039/C7NR02943H
38. R. Muszynski and B. Seger, *J. Phys. Chem. C*, **112**, 5263 (2008); https://doi.org/10.1021/jp800977b
39. J. Balapanuru, J.-X. Yang, S. Xiao, Q. Bao, M. Jahan, L. Polavarapu, J. Wei, Q.H. Xu and K.P. Loh, *Angew. Chem. Int. Ed.*, **49**, 6549 (2010); https://doi.org/10.1002/anie.201001004
40. S. Santhoshkumar, K. Velmurugan, J. Prabhu, G. Radhakrishnan and R. Nandhakumar, *Inorg. Chim. Acta*, **439**, 1 (2016); https://doi.org/10.1016/j.ica.2015.09.030
41. J. Prabhu, K. Velmurugan, A. Raman, N. Duraipandy, S. Easwaramoorthi M.S. Kiran and R. Nandhakumar, *Sens. Actuators B Chem.*, **238**, 306 (2017); https://doi.org/10.1016/j.snb.2016.07.018
42. K. Velmurugan, S. Mathankumar, S. Santoshkumar, S. Amudha and R. Nandhakumar, *Spectrochim. Acta A Mol. Biomol. Spectrosc.*, **139**, 119 (2015); https://doi.org/10.1016/j.saa.2014.11.103
43. J. Prabhu, K. Velmurugan and R. Nandhakumar, *Anal. Chem.*, **70**, 943 (2015); https://doi.org/10.1134/S1061934815080134
44. K. Velmurugan and R. Nandhakumar, *J. Lumin.*, **162**, 8 (2015); https://doi.org/10.1016/j.jlumin.2015.01.039
45. J. Prabhu, K. Velmurugan and R. Nandhakumar, *J. Lumin.*, **145**, 733 (2014); https://doi.org/10.1016/j.jlumin.2013.08.056